

Electrical relaxation dynamics in TiO₂ – polymer matrix composites

G. A. Kontos¹, A. L. Soulintzis¹, P. K. Karahaliou^{1,2}, G. C. Psarras², S. N. Georga¹,
C. A. Krontiras^{1*}, M. N. Pisanias¹

¹Department of Physics, University of Patras, 26504 Patras, Greece

²Department of Materials Science, University of Patras, 26504 Patras, Greece

Received 27 July 2007; accepted in revised form 20 September 2007

Abstract. Polymer matrix-TiO₂ composites were prepared in three different filler concentrations. The electrical relaxation dynamics as well as the electrical conductivity of all samples were examined by means of Broadband Dielectric Spectroscopy (BDS) over a wide frequency and temperature range. The recorded relaxation response includes contributions from both the polymer matrix and the reinforcing phase. Two relaxation modes (β and γ) are observed in the low temperature region, which are attributed to the re-orientation of polar side groups of the matrix and rearrangement of small parts of the polymeric chain respectively. The α -relaxation and the Maxwell-Wagner-Sillars effect (MWS), attributed to the glass-rubber transition of the polymeric matrix and to interfacial polarization phenomena respectively, are observed in the high temperature region. These two mechanisms are superimposed, thus a computer simulation procedure was followed in order to distinguish them. MWS effect becomes more pronounced with increasing concentration of the filler following an Arrhenius behaviour. The relaxation frequencies corresponding to α -mode follow the Vogel-Tamann-Fulcher (VTF) equation. An additional relaxation mode is recorded at relatively high temperatures and high frequencies. Its occurrence and dynamics are related to the presence and the concentration of the filler. Finally, the Direct Current (DC) conductivity follows the VTF equation.

Keywords: polymer composites, particulate filler, polar oxide, dielectric spectroscopy

1. Introduction

Recently polymer matrix – ceramic filler composites receive increased attention due to their interesting electrical and electronic properties. Integrated decoupling capacitors, angular acceleration accelerometers, acoustic emission sensors and electronic packaging are some potential applications [1, 2]. Furthermore, electrical properties such as dielectric permittivity can be suitably adjusted, simply by controlling the type and the amount of ceramic inclusions. Ceramic materials are typically brittle, possess low dielectric strength and in many cases are difficult to be processed requiring high temperatures. On the other hand, polymers are flex-

ible, can be easily processed at low temperatures and exhibit high dielectric breakdown fields [3]. Integrating two complementary materials in a new composite structure, results in a novel material system, the performance of which is expected to be superior in comparison to the corresponding of the constituent phases. Composite materials of an amorphous polymeric matrix and fine ceramic particles are considered as heterogeneous disordered systems. Their electrical performance is directly related to the permittivities and conductivities of their constituents, the volume fraction of the filler and the size and shape of its particles. Titanium dioxide has been the subject of many studies

*Corresponding author, e-mail: krontira@physics.upatras.gr
© BME-PT and GTE

because of its remarkable optical and electronic properties [4–6]. It can be crystallized in three distinct structures, which are known as rutile, anatase and brookite. Epoxy resins are considered as a common and successful polymer matrix for the fabrication of composite materials due to their good adhesion with reinforcing elements, enhanced thermal stability, resistance to chemical attack and resistance to degradation under the influence of corrosive environment [7–11].

In the present study, the dielectric properties of composite systems consisting of an epoxy resin and ceramic titanium dioxide particles are investigated by means of Broadband Dielectric Spectroscopy (BDS) in a wide temperature range.

2. Experimental details

2.1. Sample preparation

Polymer matrix – ceramic TiO₂ composites were prepared in three different concentrations, namely 10 phr (parts per hundred), 30 phr and 50 phr. For the preparation of the samples a commercially available low viscosity epoxy resin (Epoxol 2004A, Neotex S.A., Athens, Greece) was used as a pre-polymer. The employed curing agent (Epoxol 2004B) operates at a slow rate allowing the addition of large quantities of the reinforcing phase. Ceramic titanium dioxide powder (Sigma-Aldrich) belongs to the rutile type with mean particle diameter less than 5 μm. The followed procedure includes mixing of the resin with the curing agent in a 2:1 (w/w) ratio. While the above systems were still in the liquid state, various amounts of the ceramic powder were added for the production of the composite samples. The initial curing took place at ambient for a week, followed by post-curing at 100°C for 4 hours. The thickness of the samples ranges from 1.5 to 2.5 mm and the diameter of all samples exceeds 30 mm.

2.2. Dielectric measurements

For the electrical characterization of the composites, BDS was employed in the frequency range of 0.1 Hz to 1 MHz, using Alpha-N Frequency Response Analyser, supplied by Novocontrol. The BDS-1200, parallel-plate capacitor with two gold-plated electrodes system, supplied also by Novocontrol, was used as test cell. The dielectric cell was electrically shielded in nitrogen gas atmosphere

and isothermal frequency scans were conducted for each of the examined specimens. Measurements were performed in the temperature range of –100°C to 150°C. The employed temperature step between successive frequency sweeps was 10°C. Temperature was controlled by the Quattro system within ±0.1°C. The instrument is interfaced to a PC for simultaneous control and automated data acquisition. The applied ac voltage used is $V_{rms} = 1.0$ V.

3. Experimental results

3.1. Low temperature region

In polymer matrix composites electrical relaxation phenomena are expected to include contributions from both the polymer matrix and the ceramic filler. Thus, the respective dielectric response is expected to include relaxations arising from phase transitions of the polymer matrix (α -relaxation), as well as faster relaxations (β , γ) attributed to reorientations and segmental motions of parts of the polymer chain. Moreover, due to the presence of the filler, interfacial phenomena (MWS effect) are expected to occur.

The recorded dielectric data could be expressed in terms of real (ϵ') and imaginary part (ϵ'') of dielectric permittivity. Nevertheless, within this work the recorded data are transformed, via Equation (1), to the electric modulus formalism. Electric modulus is defined as the inverse quantity of complex permittivity:

$$M^* = \frac{1}{\epsilon^*} = \frac{1}{\epsilon' - j\epsilon''} = \frac{\epsilon'}{\epsilon'^2 + \epsilon''^2} + j \frac{\epsilon''}{\epsilon'^2 + \epsilon''^2} = M' + jM'' \quad (1)$$

where M' is the real and M'' the imaginary part of electric modulus respectively.

This formalism is used because it excludes phenomena such as electrode polarization and space charge injection which lead to high values of permittivity and conductivity especially at high temperatures and low frequencies. Consequently, it allows the better representation of the MWS effect in the low frequency region. Extended arguments for the resulting benefits of this formalism are discussed elsewhere [12, 13].

M' versus frequency as well as M'' versus frequency, in the low temperature region (–100 to

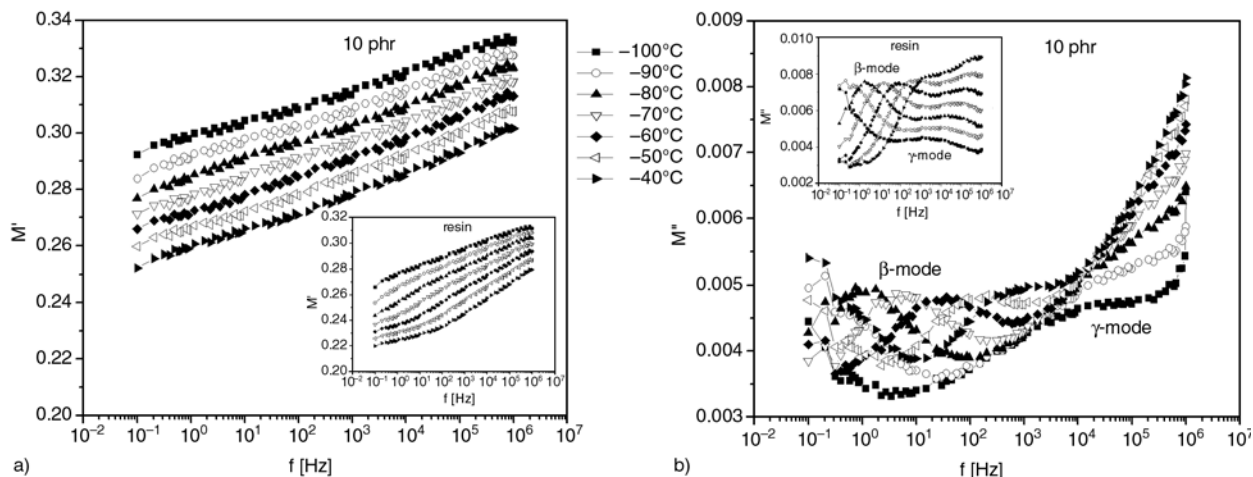


Figure 1. Real (a) and imaginary (b) part of electric modulus versus frequency for the specimen with 10 phr, in the low temperature region. Insert: Respective results for the pure epoxy specimen

–40°C), of the composite with 10 phr in TiO₂ are presented in Figures 1a and 1b respectively. Two, relatively weak, relaxation modes are recorded. These two relaxations are assigned as β- and γ-mode and they become evident via the corresponding loss peaks in the M'' spectrum. Both relaxations are originated from the pure resin, as shown in the insert of Figure 1, where the corresponding curves for the pure resin specimen, are presented. Moreover, since both processes are fast they are attributed to restricted local motions of the polymer chain i. e. re-arrangement of small parts of the polymer chain (γ-mode) and re-orientation of polar side groups (β-mode). The results suggest that the increase in concentration of ceramic TiO₂ slightly modifies the isothermal spectra of electric modulus. Specifically in the dielectric spectra, at low temperatures, of the composite with 10 phr in

TiO₂ only β-mode is clearly recorded. Elevated values of the imaginary part of electric modulus obstruct recording of the faster mechanism (γ-relaxation). Similar spectra, in the low temperature region, were obtained for the composites with 30 and 50 phr in TiO₂.

3.2. High temperature region

Plots of M' versus frequency as well as M'' versus frequency, in the high temperature region (20 to 150°C), of the composite with 10 phr in TiO₂ are presented in Figures 2a and 2b respectively. In the high temperature region, the spectrum is dominated by the presence of α-mode. This mode, which is recorded in the same frequency range as in the case of the pure resin (insert of Figure 2) is related to the glass rubber transition of the polymer

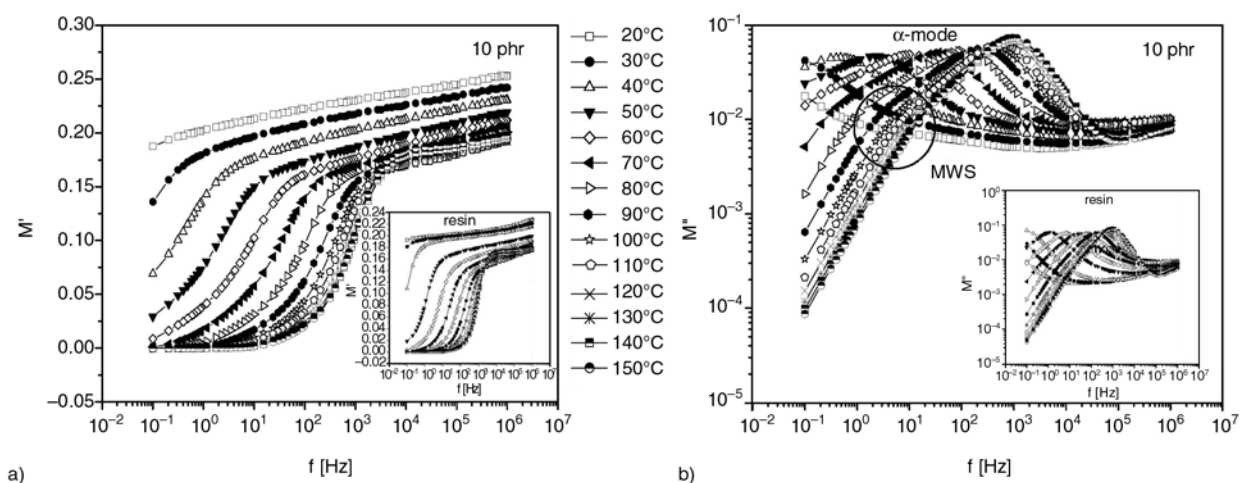


Figure 2. Real (a) and imaginary (b) part of electric modulus versus frequency for the specimen with 10 phr, at high temperatures. Insert: Respective results for the pure epoxy specimen

matrix. Peaks' position shifts to higher frequencies with increasing temperature, while the shape and magnitude of the formed peaks remain rather constant from 40 to 90°C. Above 90°C peaks' magnitude increases and the shift rate of maxima loci is reduced.

For the composite with 10 phr in TiO₂ an additional process, absent in the spectrum of pure resin, can be detected in the low frequency edge, below α -relaxation. This process which is evident as a shoulder in the log-log spectra of M'' (Figure 2b), at any given temperature, is slower than α -relaxation. It is reasonable to suggest that interfacial phenomena are responsible for the occurrence of this mode. Interfacial polarization or MWS effect [14–16] is a relaxation process appearing in heterogeneous systems due to accumulation of charges at the interfaces of the system. The origin of these non-bounded charges arises from the stage of specimen preparation. At the matrix/particle interface charges form large dipoles, which are not able to follow simultaneously the alternation of the applied electric field. In the electric modulus presentation, the intensity of loss peaks is expected to decrease with increasing filler content. This becomes evident by simply comparing the results from the pure resin and those of the samples with 10 phr in TiO₂ (Figure 2b).

Pronounced MWS effect characterizes composite systems exhibiting high electrical heterogeneity between their phases. Typical examples of such systems are insulating matrix – conductive inclusions composites [17, 18]. The examined systems are consisting of titanium dioxide, which is a wide band gap semiconductor, and a typical insulating

thermoset polymer such as epoxy resin. Thus significant variation between the values of conductivity of the two constituent phases does not exist and consequently a remarkable MWS effect is not expected to occur. Dielectric spectra of Figure 2b are in accordance with previous remarks since only a weak interfacial polarization is recorded.

In the high frequency region, above α -mode, another process is evident as a tail in the log-log spectra of composite with 10 phr in TiO₂. The occurrence of this mode becomes more pronounced in composites with 30 and 50 phr in TiO₂ as shown in Figure 3.

In Figures 3a and 3b the imaginary part of electric modulus (M'') versus frequency is plotted in a log-log representation, for the composites with 30 and 50 phr in TiO₂, respectively. Both MWS effect and α -mode are detected. The high frequency relaxation process which is absent in the dielectric spectrum of the pure matrix and not completely formed in the specimen with 10 phr, is now recorded. Thus the appearance of this process is strongly affected by the filler's concentration and should be attributed to the ceramic filler itself. Its location is intermediate in the dielectric spectra, lying between the fast (local modes) and the slow (α -mode and MWS effect) processes, so for reasons of brevity, it would be called further on, as Intermediate Dipolar Effect (IDE).

3.3. AC electrical conductivity

The Alternating Current (AC) conductivity σ' of all samples has been calculated from the dielectric losses according to the Equation (2):

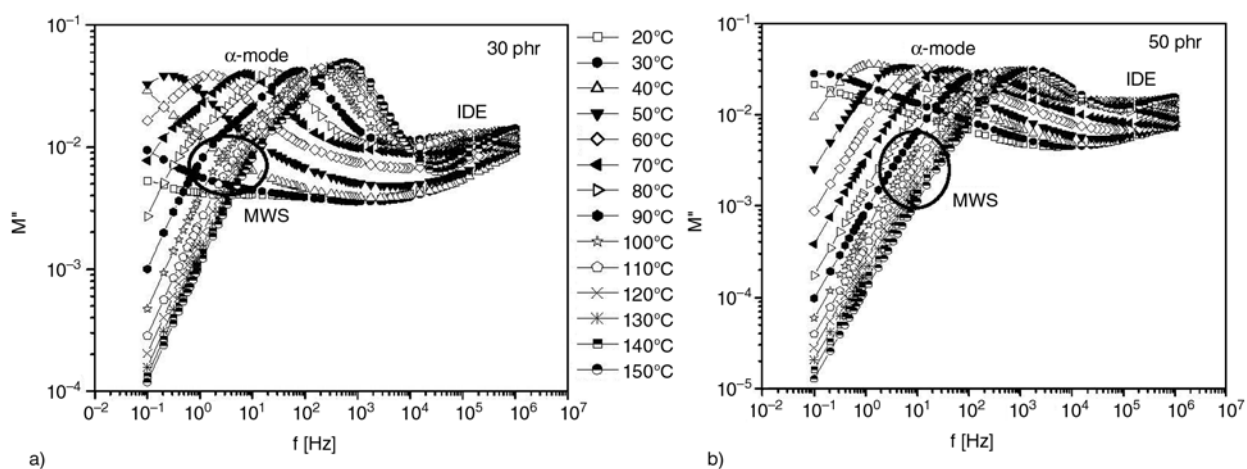


Figure 3. Imaginary part of electric modulus (M'') versus frequency for the specimens with (a) 30 phr and (b) 50 phr in TiO₂, at high temperatures

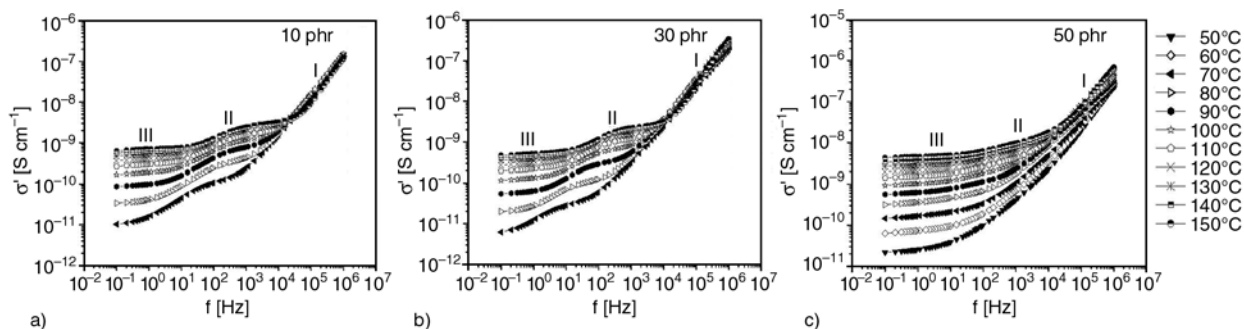


Figure 4. The real part of electrical conductivity (σ') versus frequency at elevated temperatures for composites with (a) 10 phr, (b) 30 phr and (c) 50 phr

$$\sigma' = \epsilon_0 \omega \epsilon'' \tag{2}$$

where $\epsilon_0 = 8.85 \cdot 10^{-12}$ F/m is the permittivity of the free space and $\omega = 2\pi f$ the angular frequency.

AC conductivity as a function of frequency is presented in Figure 4, at the high temperature region, for the composites with 10, 30 and 50 phr in TiO_2 . For all the tested specimens an increase of conductivity σ' with temperature is observed especially at low frequencies. The dependence of electrical conductivity with frequency can be divided into distinct regions implying the existence of different dissipated effects [19]. In the high frequency region (I), conductivity increases with increasing frequency following the universal dielectric response law, $\sigma' = A\omega^n$, where n was found to be very close to 1. In this region a weak dependence of the conductivity with temperature is evident. In the low frequency region (III) a leveling off of the electrical conductivity is observed. This corresponds to the DC conductivity of the samples, which increases significantly with increasing temperature. In the intermediate region (II), dipolar relaxation

processes are present, the intensity of which is dependant upon filler content. Recalling dielectric data from Figures 2 and 3, two modes could be considered as responsible for the observed behaviour, in the specific region, namely MWS and α -mode. However, in the AC conductivity formalism, resolve and quantification of the relative contributions can not be carried out.

4. Discussion

Figure 5 provides isothermal plots of the imaginary part of the electric modulus (M'') as a function of frequency, at two different temperatures, namely -80 and 120°C , for the specimens with 10, 30 and 50 phr in TiO_2 content.

In Figure 5a, both low temperature relaxation processes, namely β -mode and γ -mode, are evident in the specimen with 10 phr. β -mode is recorded in all tested samples and appears not to be influenced by the filler's concentration. On the contrary, γ -mode becomes weaker as the filler's concentration increases and is finally obstructed, in the spectra of 30 and 50 phr.

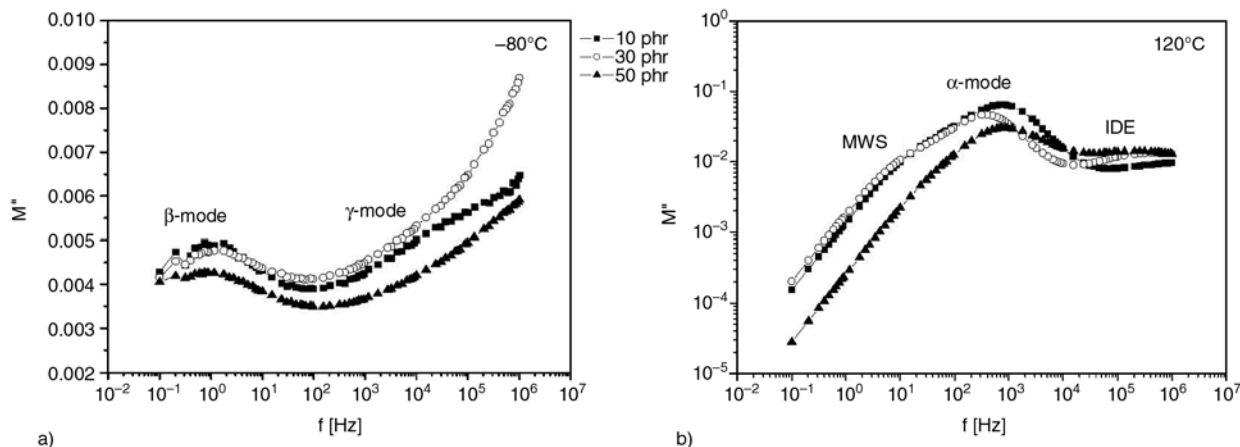


Figure 5. Imaginary part of electric modulus (M'') versus frequency for all composites specimens at (a) -80°C and (b) 120°C

In Figure 5b, α -mode is recorded in the middle of the frequency region forming a clear peak. The intensity of the peak is varies with filler's content. At the low and high frequency edges of the dielectric response spectra interfacial polarization phenomena (MWS effect) and IDE-mode are recorded respectively. IDE becomes stronger in the composites of 30 and 50 phr in TiO₂. The physical origin of IDE process cannot be ascribed unambiguously. The fact that it is detected in specimens with increased concentration of TiO₂ implies that its source should be sought in the polarization effects of the ceramic filler. TiO₂ is dielectrically anisotropic material, its unit cell attains tetragonal crystal structure and the static values of dielectric permittivity in the perpendicular and the lateral direction differ significantly [20]. Titanium oxide is classified as a polar oxide, exhibiting transitions between crystal structures with varying symmetry [21]. The local environment of the titanium sites in rutile is similar to that in barium titanate. The titanium site is surrounded by an octahedron of oxygen sites with a titanium-oxygen distance of $\sim 2\text{\AA}$ [20]. The low symmetry of the unit cell of titanium dioxide, at room temperature, and the similarities to barium titanate is a strong indication that spontaneous polarization might be occurring in TiO₂. In that case, polarization effects might be relaxing under the influence of an external alternating electric field. The influence of temperature upon the distance of sites in the unit cell of TiO₂ might assert a more symmetrical structure, where the redistribution of polarizabilities will produce zero net polarization. If so, a disorder to order, or in other words ferroelectric to paraelectric transition will take place at a critical temperature. However, in order to verify these initial indications more experimental work is necessary to be carried out.

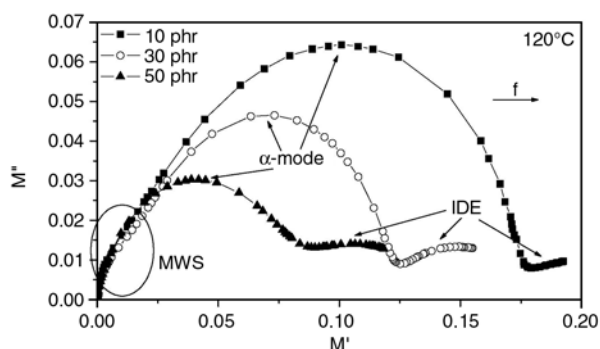


Figure 6. Cole-Cole plots for all composite specimens at 120°C

The high temperature relaxation processes are also shown in the Cole-Cole representation of Figure 6. Apart from the semicircle corresponding to α -mode, MWS relaxation is also present in the low frequency edge. This fact is demonstrated by the asymmetry of the respective curves in the low frequency region where a hump is observed. The coincidence of the beginning of semicircles with the origin of the graph is a clear indication that no other relaxation process is present, at lower frequencies, in all studied composite systems. Moreover, the variation of the semicircles radius, corresponding to the α -mode, indicates that α -mode is influenced by the filler's concentration. Furthermore, at the high frequency end, experimental results from the composites with 30 and 50 phr contents in TiO₂ form a suppressed semicircle reflecting the presence of IDE-mode.

Aiming to analyze the contribution of the three mechanisms, which are present at elevated temperatures, curves of $\log M''$ versus $\log f$ are fitted using a multi-peak fitting procedure. As an example, the fitting procedure employed for the specimen with 30 phr in TiO₂ is shown in Figure 7. The experimental data are fitted using, as first approximation, three Debye-type processes. The experimental data are satisfactorily described by the solid line which is a superposition of the three Debye-type relaxation processes corresponding to each of the experimentally determined modes (dashed lines). Debye-type processes are characterized by a single relaxation time, which can be easily evaluated by the abscissa of loss maxima. Obtained results are given in Table 1. The influence of the filler content on relaxation dynamics, as expressed by the evalu-

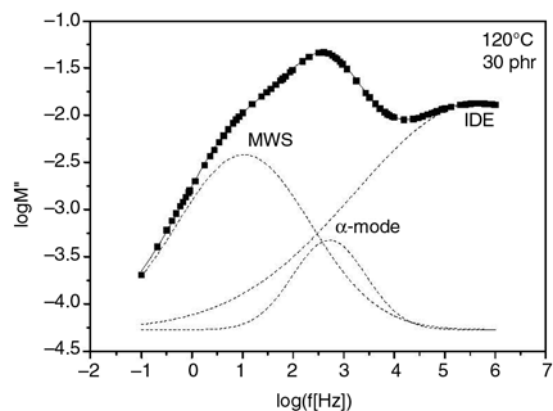


Figure 7. Fitting procedure for the composite with 30 phr in TiO₂ at 120°C. The experimental data are fitted via the superposition of three Debye-type processes

Table 1. Evaluated relaxation times at 120°C

Sample	τ [ms]		
	MWS	α -mode	IDE
Epoxy + 10 phr TiO ₂	45.31	0.15	–
Epoxy + 30 phr TiO ₂	7.76	0.29	0.2·10 ⁻³
Epoxy + 50 phr TiO ₂	0.49	0.22	0.03·10 ⁻³

ated relaxation times, appears to be more pronounced in the MWS and IDE effects. In both cases relaxation times decrease with increasing filler’s content, implying that both processes are facilitated with the increase of TiO₂ content. Taking into account the frequency-temperature superposition it can be concluded that MWS and IDE effects appear at lower temperature range as the TiO₂ content increases. On the other hand the relaxation times of α -mode do not show any particular trend with the variation of filler’s content. However, the validity of this conclusion is limited since the glass/rubber relaxation process deviates from a pure Debye mechanism.

The temperature dependence of loss peak position for all the examined systems and for all three relaxation processes at elevated temperatures is depicted in Figure 8. MWS and IDE modes exhibit an Arrhenius type behaviour in all concentrations according to the Equation (3):

$$f_{max} = f_0 \exp\left(-\frac{E_A}{k_B T}\right) \quad (3)$$

where f_0 is a pre-exponential factor, E_A the activation energy, k_B the Boltzmann constant, and T the temperature in K. The temperature dependence of

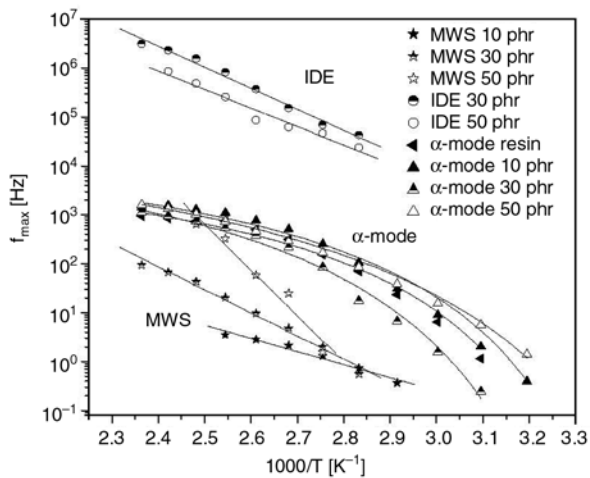


Figure 8. The dependence of relaxation frequencies with the reciprocal temperature at elevated temperatures, for all measured samples

Table 2. Activation energies and VTF parameters for all the tested specimens

	MWS	α -mode		IDE
	E _A [eV]	T ₀ [K]	B [K]	E _A [eV]
Epoxy	–	280	395	–
Epoxy + 10 phr TiO ₂	0.53	275	430	–
Epoxy + 30 phr TiO ₂	0.94	280	545	0.85
Epoxy + 50 phr TiO ₂	1.86	285	595	0.75

α -relaxation can be described by the Vogel-Tamann-Fulcher equation (4) [22–24]:

$$f_{max} = f_0 \exp\left(-\frac{B}{T - T_0}\right) \quad (4)$$

where f_0 is a pre-exponential factor, B a constant (being a measure of the activation energy), and T_0 Vogel temperature or ideal glass transition temperature. This equation considers that relaxation rate increases rapidly at lower temperatures because of the reduction of free volume.

Table 2 summarizes the obtained results for the activation energies of MWS and IDE effects as well as the VTF parameters T_0 and B .

The dependence of the Direct Current (DC) electrical conductivity σ_{DC} (σ' at 0.1 Hz) with reciprocal temperature is shown in Figure 9 for all the composites. DC conductivity remains rather constant for composites with 10 and 30 phr. This is not a surprising behaviour taking into account the insulating nature of both the inclusion and the matrix. A slight increase is observed only for the composite with 50 phr.

DC conductivity values follow the Vogel-Tamann-Fulcher equation (5):

$$\sigma_{DC} = \sigma_0 \exp\left(-\frac{B}{T - T_0}\right) \quad (5)$$

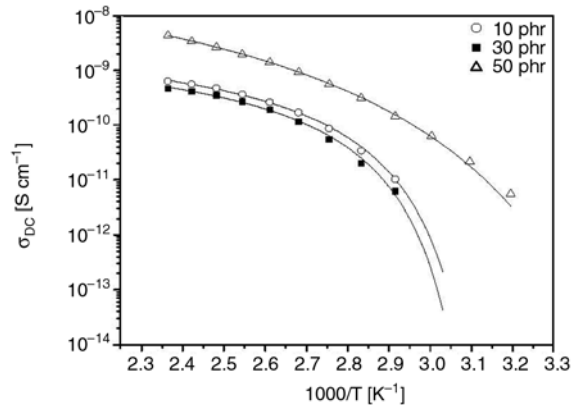


Figure 9. DC electrical conductivity as a function of reciprocal temperature

Table 3. VTF parameters concerning the temperature dependence of DC conductivity at the examined composites

	B [K]	T₀ [K]
Epoxy + 10 phr TiO ₂	196	306
Epoxy + 30 phr TiO ₂	188	313
Epoxy + 50 phr TiO ₂	569	259

where σ_0 pre-exponential factor, B a parameter related to the activation energy and T_0 is the Vogel temperature. The experimental data are satisfactorily fitted by VTF equation (solid lines) and fitting parameters are listed in Table 3.

4. Conclusions

The dielectric response of polymer composites consisting of an epoxy resin matrix and rutile TiO₂ ceramic filler has been studied in the frequency range 0.1 Hz–1 MHz and temperatures from –100 to 150°C. The relaxation phenomena recorded include contributions from both the polymeric matrix and the reinforcing phase. At low temperatures, two distinct relaxation processes, namely β - and γ -mode, were detected in all composites and originate from the pure resin. Both dielectric processes are attributed to local motions resulting from reorientations of polar side groups and small segments of the polymer chain. At high temperatures three additional relaxation processes were detected. From lower to higher frequencies at constant temperature, they are attributed to interfacial polarization phenomena (MWS effect), glass/rubber transition, and to relaxing polarization (IDE) of the TiO₂ ceramic particles respectively. MWS effect becomes stronger with increasing filler's concentration and IDE becomes more pronounced at the concentrations of 30 and 50 phr in TiO₂. MWS and IDE relaxations exhibit an Arrhenius type dependence with temperature while α -mode follows VTF model. Relaxation times and activation energies for all high temperature modes were calculated. The DC electrical conductivity of all samples was evaluated at 0.1 Hz, where a leveling off of the corresponding curves is observed at the relatively high temperatures. DC electrical conductivity increases with increasing temperature following the VTF model. Finally, the existence of a self-relaxing polarization mechanism in ceramic

TiO₂ composites can be exploited for the design of functional polymer matrix systems.

Acknowledgments

This work was partially supported by the General Secretariat for Research and Technology (GSRT) of Greece in the framework of Joint Research and Technology Programs between Greece and Tunisia (project code 121-e).

References

- [1] Chahal P., Tummala R. R., Allen M. G., Swaminathan M.: A novel integrated decoupling capacitor for MCM-L technology. *IEEE Transactions on Components Packaging and Manufacturing Technology, Part B: Advanced Packaging*, **21**, 184–193 (1998).
- [2] Dias C. J., Igreja R., Marat-Mendes R., Inacio P., Marat-Mendes J. N., Das-Gupta D. K.: Recent advances in ceramic-polymer composite electrets. *IEEE Transactions on Dielectrics and Electrical Insulation*, **11**, 35–40 (2004).
- [3] Bai Y., Cheng Z.-Y., Bharti V., Xu H. S., Zhang Q. M.: High-dielectric-constant ceramic-powder polymer composites. *Applied Physics Letters*, **76**, 3804–3806 (2000).
- [4] Bhuvanesh N. S. P., Gopalakrishnan J.: Solid-state chemistry of early transition-metal oxides containing d⁰ and d¹ cations. *Journal of Materials Chemistry*, **7**, 2297–2306 (1997).
- [5] Linsebigler A. L., Lu G., Yates J. T.: Photocatalysis on TiO₂ surfaces: Principles, mechanisms, and selected results. *Chemical Reviews*, **95**, 735–758 (1995).
- [6] Oehrlein G. S.: Oxidation temperature-dependence of the DC electrical-conduction characteristics and dielectric strength of thin TA205 films on silicon. *Journal of Applied Physics*, **59**, 1587–1595 (1986).
- [7] Varma I. K., Gupta V. G.: Thermosetting resin-properties. In: 'Comprehensive Composite Materials' (eds.: Talreja R., Manson J-A. E., Kelly A., Zweben C.) Elsevier, Amsterdam, Vol 2, chapter 2.01, p. 2–18 (2000).
- [8] Hull D., Clyne T. W.: An introduction to composite materials. Cambridge University Press, Cambridge (1996).
- [9] Daniel I. M., Ishai O.: Engineering mechanics of composite materials. Oxford University Press, Oxford (1994).
- [10] Schwartz M. M.: Composite materials handbook. McGraw-Hill, New York (1984).
- [11] Ellis B.: Chemistry and technology of epoxy resins. Blackie Academic and Professional, London (1993).

- [12] Tsangaris G. M., Psarras G. C., Kouloumbi N.: Electric modulus and interfacial polarization in composite polymeric systems. *Journal of Materials Science*, **33**, 2027–2037 (1998).
- [13] Psarras G. C., Manolakaki E., Tsangaris G. M.: Electrical relaxations in polymeric particulate composites of epoxy resin and metal particles. *Composites, Part A: Applied Science and Manufacturing*, **33**, 375–384 (2002).
- [14] Macedo P. B., Moynihan C. T., Bose R.: The role of ionic diffusion in polarization in vitreous ionoc conductors. *Physics and Chemistry of Glasses*, **13**, 171–179 (1972).
- [15] Bakr A. A., North A. M.: Charge carriers hopping in poly(arylenevinyl-enes). *European Polymer Science*, **13**, 799–803 (1977).
- [16] Starkweather H. W., Avakian P.: Conductivity and electric modulus in polymers. *Journal of Polymer Science, Part B: Polymer Physics*, **30**, 637–641 (1992).
- [17] Tsangaris G. M., Psarras G. C.: The dielectric response of a polymeric three-component composite. *Journal of Materials Science*, **34**, 2151–2157 (1999).
- [18] Psarras G. C., Manolakaki E., Tsangaris G. M.: Dielectric dispersion and ac conductivity in-iron particles loaded-polymer composites. *Composites, Part A: Applied Science and Manufacturing*, **34**, 1187–1198 (2003).
- [19] von Hippel A. R.: *Dielectrics and waves*. Artech House, Boston (1995).
- [20] Parker R. A.: Static dielectric constant of rutile (TiO₂), 1.6-1060K. *Physical Review*, **124**, 1719–1722 (1961).
- [21] Kim J. Y., Jung H. S., No J. H., Kim J. R., Hong K. S.: Influence of anatase-rutile phase transformation on dielectric properties of sol-gel derived TiO₂ thin films. *Journal of Electroceramics*, **16**, 447–451 (2006).
- [22] Vogel H.: Das Temperaturabhängigkeitgesetz der Viskosität von Flüssigkeiten. *Zeitschrift für Physik*, **22**, 645–646 (1921).
- [23] Tammann G., Hesse W.: Die Abhängigkeit der Viskosität von der Temperatur bei unterkühlten Flüssigkeiten. *Zeitschrift für Anorganische und Allgemeine Chemie*, **156**, 245–257 (1926).
- [24] Fulcher G. S.: Analysis of recent measurements of the viscosity of glasses. *Journal of the American Ceramic Society*, **8**, 339–355 (1925).